Int J Earth Sci (Geol Rundsch) (2005) 94: 369–384
DOI 10.1007/s00531-004-0460-1

ORIGINAL PAPER

Thorsten Geisler · Roland Vinx
Nergui Martin-Gombojav · Robert T. Pidgeon

Ion microprobe (SHRIMP) dating of detrital zircon grains from quartzites of the Eckergneiss Complex, Harz Mountains (Germany): implications for the provenance and the geological history

Received: 18 May 2004 / Accepted: 5 November 2004 / Published online: 13 April 2005

Abstract The Eckergneiss Complex (EGC) is a geologically unique medium- to high-grade metamorphic unit within the Rhenohercynian domain of the Mid-European Variscides. A previously, poorly defined conventional lower U–Pb intercept age of about 560 Ma from detrital zircons of metasedimentary rocks has led to speculations about an East Avalonian affinity of the EGC. In order to unravel the provenance and to constrain the age of the sediment protolith, we carried out sensitive high-resolution ion microprobe U–Pb analyses on detrital zircons from five different EGC quartzite occurrences. The obtained age spectrum indicates a SW Baltica provenance of the detritus. Sveconorwegian ages between 0.9–1.2 Ga are particularly well represented by analyses from metamorphic recrystallization/alteration zones penetrating into igneous zircon. Cadomian (Pan-African) ages, which might reflect a metamorphic event, could not be substantiated. Instead, zircons of igneous origin yielded concordant Lower Devonian and Silurian ages of 410 ± 10, 419 ± 10, and 436 ± 6 Ma (1σ), implying that sedimentation of the EG protolith must have taken place after 410 ± 10 Ma. The lower age limit of the EGC metamorphism is constrained by 295 Ma intrusion ages of the adjacent, nonmetamorphosed Harzburg Gabbronorite and Brocken Granite. Sedimentation and metamorphism must thus have taken place between about 410 Ma and 295 Ma. Given that this time span coincides with most of the sedimentation within the virtually nonmetamorphosed (lowest grade) Rhenohercynian in the Harz Mountains, including the direct vicinity of the EGC, along with the high-grade metamorphism, the EGC can hardly be seen as uplifted local basement. A possible candidate for the root region is an easterly, concealed marginal segment of the Rhenohercynian domain of the Variscides, which is tectonically overridden and suppressed by the Mid-German Crystalline Rise during continent collision. However, based on the concept of strike-slip movement of Variscan terranes with different P–T–t histories as a result of postaccretion intraplate deformation, the EGC could also represent a fault-bounded complex with an origin located far east or south east of the present location.

Keywords Eckergneiss · Variscides · Harz · SHRIMP · Zircon · Provenance · Baltica

T. Geisler (✉)
Mineralogisches Institut,
Universität Münster,
Corrensstr. 24,
48149 Münster, Germany
E-mail: tgeisler@nwz.uni-muenster.de

R. Vinx · N. Martin-Gombojav
Mineralogisch-Petrographisches Institut der Universität Hamburg,
Grindelallee 48, 20146 Hamburg,
Germany

R. T. Pidgeon
School of Applied Geology,
Curtin University of Technology,
GPO Box U 1987, Perth,
6845, WA, Australia

Introduction

The Eckergneiss Complex (EGC) in the Harz Mountains (Germany) is a high-grade polymetamorphic crustal segment within the Rhenohercynian domain of the Mid-European Variscides (Fig. 1). The high-grade metamorphism of the EGC is a matchless feature within the low-grade Rhenohercynian domain, raising questions about its geological history, which, in turn is important to our understanding of the geodynamic evolution of the Variscan orogenic belt. A conventional lower intercept U–Pb age of about 560 Ma from detrital zircon grains, interpreted to reflect the timing of the main metamorphism (Bauman et al. 1991), suggests that the EGC represents the oldest geological unit of the Harz Mountains. This age has led to controversial speculations about the tectonic setting of the EGC. Bankwitz (1995) suggested that the EGC represents a Cadomian–Caledonian tectonic flake formed during the collision of

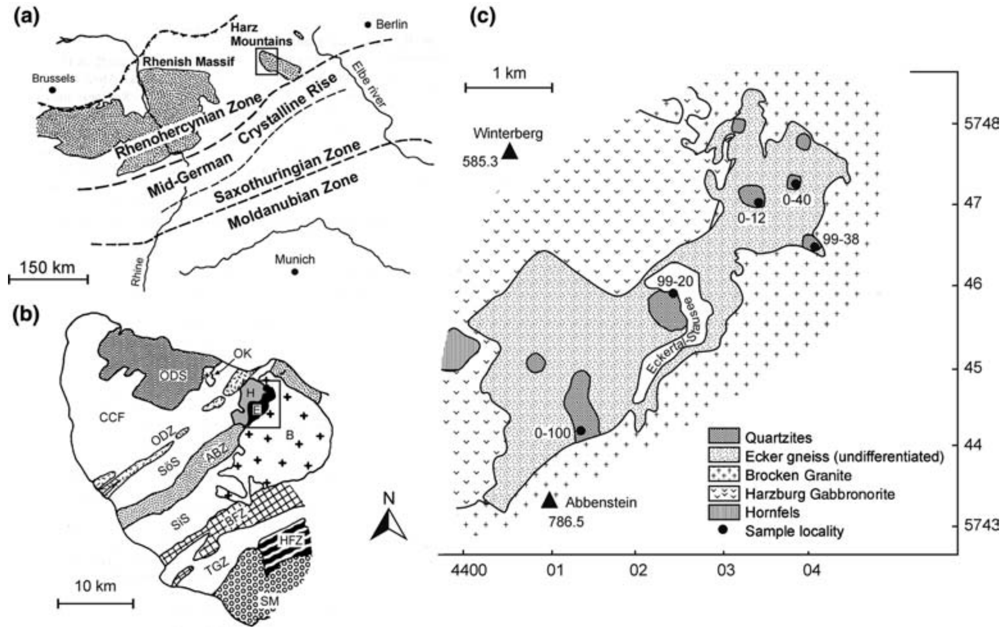

Fig. 1 **a** Subdivision of the Mid-European Variscides after Franke (1989). **b** Geological subdivision of the Upper and Middle Harz (after Mohr 1978): *HFZ* Harzgeröder fold zone, *TGZ* Tanne greywacke zone, *BFZ* Blankenburger fold zone, *SiS* Sieber syncline, *SM* South Harz syncline, *B* Brocken Granite, *E* Eckergneiss Complex, *H* Harzburg Gabbronorite, *OK* Oker Granite, *ABZ* Acker–Bruchberg zone, *ODZ* Upper Harz diabase range, *SöS* Söse syncline, *CCF* Clausthaler Culm fold zone, *ODS* Devonian anticline of the Upper Harz. **c** Simplified geological map of the Eckergneiss Complex with quartzite occurrences and sample localities

Gondwana with East Avalonia. Other authors favored a model that explains the EGC as being uplifted upon the intrusive ascent of the magmas of the adjacent Brocken Granite and the Harzburg Gabbronorite (Baumann et al. 1991; Franz et al. 1997). Based on the ''Cadomian'' (Pan-African) age Franz et al. (1997) further speculated that the EGC belongs to the East Avalonian terrane. Whereas these models agree in assuming that the EGC is an allochthonous enclave within the Rhenohercynian domain, Franzke (2001) has suggested that the EGC may represent a semi-autochthonous outcrop topping a crystalline high located between the Oberharzer Diabaszug (Upper Harz diabase belt) and the Blankenburger Faltenzone (Blankenburg fold zone; Fig. 1b).

The present study was initially based on the premise of a ''Cadomian'' (Pan-African) metamorphic age. The original objectives were to identify the assumed pre-Cadomian provenance of the sedimentary Eckergneiss protolith assemblage, to constrain its deposition age, and, accordingly, the geotectonic position of the EGC by characterizing the age structure of the detrital zircon component of five quartzite occurrences. Zircon is of particular value for provenance studies, since it is chemically and physically resistant and not liable to destruction during the weathering and sedimentary cycle. Furthermore, zircon forms predominantly in felsic-intermediate igneous and metamorphic rocks, and thus records major crust-forming events that characterize potential source areas. However, zircon crystals that have accumulated a certain amount of self-irradiation structural damage or those that are rich in rare earth elements are prone to react with geological fluids, resulting in inward penetrating alteration or recrystallization zones that are usually characterized by a disturbed U–(Th)–Pb system (e.g., Black et al. 1986; Geisler et al. 2001, 2002, 2003a, 2003b, 2003c; Schaltegger et al. 1999; Tomaschek et al. 2003; Vavra et al. 1996, 1999). In addition, more than one growth generation may be preserved in single zircon grains (e.g., Black et al. 1986; Geisler and Schleicher 2000). Based on these grounds, multi-phase zircon crystals are common in metamorphic terranes. We note here that Anthes and Reischmann (2001) mentioned that their ''efforts to date the formation age of the EGC or its source using single zircon analyses failed so far''. In consequence, imaging techniques and microanalytical tools must be applied to unravel the internal structures and their age relationships, to obtain geologically interpretable age data. In the present study, we used cathodoluminescence imaging to visualize the internal structures, which were dated in situ by the sensitive high-resolution ion microprobe (SHRIMP) technique. By doing this, we also hoped to be able to date the metamorphic events within the EGC.

Regional setting and basic petrographical features

The EGC is located within the Harz Mountains in central Germany (Fig. 1), which represent a tectonically uplifted segment of the Variscan orogenic belt of central Europe. The Variscan belt is a very complex conglomeration of small crustal blocks of different P–T–t histories that were juxtaposed along strike-slip and detachment systems. The belt is commonly divided into four tectono-stratigraphic units from NW to SE (e.g., Franke 1989): the Rhenohercynian Zone, Mid-German Crystalline Rise (MGCR), the Saxothuringian Zone, and the Moldanubian Zone (Fig. 1a). The Harz Mountains belong to the Rhenohercynian domain and reflect a long evolution of sedimentary, erosional, tectonic, and magmatic processes. The Harz essentially comprises diagenetic and low-grade metamorphosed sedimentary rocks (Friedel et al. 1995) of Ordovician to Upper Carboniferous age. Major basaltic (spilitic) intercalations occur in Middle Devonian and Lower Carboniferous shales and slates, commonly as piles of pillow lavas. Granitoid and gabbroic plutonic rocks form ca. 295-Ma old (Baumann et al. 1991), high-level intrusions within Devonian and Lower Carboniferous country rocks. Significant metamorphic imprint is confined to thermal aureoles around these intrusions.

In Devonian times, the palaeogeographic position of the present Harz area was determined by its affiliation to the Rhenohercynian domain between the Old Red continent (Laurussia) to the north and the MGCR to the southeast. At that time, pelitic, psammitic, and carbonate sediments were deposited, now represented by slates, sandstones, and limestones, which are mainly exposed in the Oberharzer Devonsattel (Upper Harz Devonian Anticline). The Lower Carboniferous constitutes most of the western and central Harz being represented by flysch series (turbiditic graywackes and shales, Fig. 1b) and the Acker–Bruchberg–quartzite (ABQ) (quartzitic sandstone, Acker–Bruchberg zone in Fig. 1b). The sedimentary strata were tectonically overprinted in the course of the last compressional (Asturian) phase of the Variscan orogenic cycle about 300 Ma ago (Mohr 1978).

The EGC represents a 7-km^2 large crustal segment that is enclosed by the high level intrusions of the Harzburg Gabbronorite and the Brocken Granite (Fig. 1c). The complex consists of pelitic and siliciclastic metasediments (e.g., quartzites, quartz-(cordierite)-feldspar granofelses, gneisses, hornfelses, and mica schists) with subordinate metabasaltic intercalations. The metasedimentary character of almost the entire EGC is indicated, for example, by a psammitic-pelitic, virtually Ca-devoid geochemistry and rare examples of preserved sedimentary depositional structures. These are thin, placer-like laminae of concentrated heavy minerals and cross bedding (Schlüter 1983, unpublished doctoral thesis).

Erdmannsdörffer (1909) has interpreted the EGC as representing a metamorphic equivalent of the ABQ, which he thought was thermally affected by the intrusions of the Brocken Granite and the Harzburg Gabbronorite. However, petrographic and petrological investigations revealed that the EGC experienced multiple metamorphic events, ranging from contact metamorphic to amphibolite and granulite-facies conditions (Franz et al. 1997; Martin-Gombojav 2003, unpublished doctoral thesis; Müller and Strauss 1985; Schlüter 1983, unpublished doctoral thesis). Franz et al. (1997) determined amphibolite- and granulite facies conditions of 560–650°C and $P >$ 0.5 GPa and 720–780°C and 0.67–83 GPa, respectively.

Whereas, the contact metamorphic event can be temporally correlated with the intrusion of the neighboring Harzburg Gabbronorite and Brocken Granite 293–297 Ma ago (Baumann et al. 1991), right at the Carboniferous/Permian border, the regional metamorphic events have not yet confidently been dated by conventional dating methods. Schoell et al. (1973) obtained a Rb–Sr whole rock isochron age of 392 ± 10 Ma[1] from various metasedimentary lithologies scattered over much of the EGC outcrop. They interpreted this datum to reflect the main metamorphism of the EGC. However, the geological significance of such an isochron remains doubtful. The same doubt applies to the lower intercept U–Pb age of about 560 Ma of Baumann et al. (1991) from euhedral and rounded detrital zircons from metasedimentary rocks within the EGC.

Franz et al. (1997) postulated that the amphibolite facies mineral assemblages were formed during a completely new metamorphic loop. However, we would like to note here that new petrographical observations from various localities of the EGC outcrop (Martin-Gombojav 2003, unpublished doctoral thesis) point to a sequence of metamorphic events in an opposite order than suggested by Franz et al. (1997). Significant in this context are the following observations: (a) poikiloblastic orthopyroxene, which is unaffected by foliation, (b) undeformed symplectites of orthopyroxene and cordierite, obviously at the expense of pyralspite garnet, and (c) no significant alteration or replacement of most of the orthopyroxenes. These features indicate that re-equilibration at granulite-facies temperatures was essentially static and followed earlier penetrative deformation, which seems to have taken place at amphibolite facies temperatures. Amphibolite-facies conditions of 650–700°C and about 0.4 GPa, which were estimated by Schlüter (1983, unpublished doctoral thesis) from kinzingites of the EGC, are in full agreement with the new petrographical observations. Additional indications of dynamic metamorphism under amphibolite-facies conditions are porphyroclasts of critical minerals such as garnet, andalusite, and cordierite (pinite) with a fine-grained foliation wrapped around them, but obviously never so with orthopyroxene. The orthopyroxene–cordierite symplectites as listed under (b) indicate an episode of postdeformational granulite-facies metamorphism. They occur in close proximity to essentially unretrograded, blocky orthopyroxene porphyroblasts, a few of which are bent by tectonic (or intrusive?) pressure.

Sample description

For the present investigation, we have chosen five quartzite samples from different localities (Fig. 1a). Samples 99-20, 0-12, and 0-100 were sampled from the east shore of the Eckertal Stausee, from the Spörenwagen, and from the south Kolför locality, respectively. Sample 99-38 was collected from the Unterer Lobenklee area, which had been mapped by Erdmannsdörffer (1909) as belonging to the ABQ formation. Recent field work and petrographic investigations, however, have

[1] Recalculated using the decay constants recommended by Steiger and Jäger (1977)

shown that the rocks of this locality exhibit high-grade metamorphism and thus clearly belong to the EGC (Martin-Gombojav 2003, unpublished doctoral thesis). Sample 0-40 was sampled from a locality in the Kleines Gierstal.

Some quartzite samples contain significant amounts of K-feldspar and plagioclase. Subordinate components are pinite, chlorite, muscovite, and a mature detrital heavy mineral population of zircon, chromite, garnet and rutile. Monazite was only found in sample 0-12. Sample 0-100 also contains newly formed tourmaline (enclosing ilmenite grains) and titanite. The detrital accessory minerals, which necessarily were deposited as independent grains, are commonly enclosed in random distribution in quartz. This feature indicates a high-metamorphic grade and clearly distinguishes the Eckergneiss quartzites from the quartzitic sandstones of the ABQ formation (Fig. 2). We also note that the detrital chrome spinel grains of all five EGC quartzite samples, analyzed by Martin-Gombojav (2003, unpublished doctoral thesis), have unusually low-Mg/(Mg $+Fe^{2+}$) values due to low-Mg concentrations. Such unusual chemical composition further discriminates the EGC quartzites not only from the quartzitic sandstones of the ABQ and from Devonian to Carboniferous sandstones and greywackes of the Harz (Fig. 3), but also from Early to Middle Devonian sandstones of the Rhenish Massif (Press 1986). The ABQ, however, also contains low-Mg chromite grains as a subordinate fraction among more abundant chromites with normal Mg-contents (Fig. 3). This indicates that the low-Mg content in the EGC chromites is inherited from a distinct though unknown source, which also contributed to the ABQ rather than being the result of processes after deposition within the EGC protolith. The metamorphism of the EGC, as might be suspected, cannot be responsible for the Mg-deficit. This conclusion is consistent with missing internal, textural features of the chromites that would indicate metamorphic alteration (Tesalina et al. 2003, and references therein).

Most of the quartzite samples of the EGC exhibit a granoblastic texture. The quartz grains are only slightly interlocked. They rarely show undulatory extinction. Some of the quartzites contain interstitial feldspar with a tendency towards poikiloblastic growth between the quartz grains. Only sample 99-20 exhibits flattened platy quartz grains with interlocked grain boundaries. This sample, as well as sample 0-12, is also foliated. The foliation in these samples is macroscopically accentuated by thin pinite-chlorite bands.

Analytical method

Ninety SHRIMP measurements on 76 zircons, separated from the five quartzite samples using heavy liquids and a magnetic separator (Fig. 1), were carried out during two 24-h analytical sessions at the WA Consortium SHRIMP II at the Curtin University of Technology in Perth (Appendix), employing the SHRIMP technique as described in DeLaeter and Kennedy (1998). The primary O_2^- beam was focused to a 25 to 40-μm diameter area onto the target zircon. The mass resolution was better than 5,200 in both sessions, which was sufficient to resolve isobaric interferences. Measured U–Pb ratios were corrected following Claoué-Long et al. (1995) from eight to ten regular analyses of the standard zircon CZ3 (Pidgeon et al. 1994) over each 24-h analytical session, resulting in $^{206}Pb/^{238}U$ calibration errors of 3.5% and 1.6 %, respectively. The isotopic ratios were further corrected for common lead using Broken Hill Pb composition and the ^{204}Pb correction method (Compston et al. 1984). Counting times were reduced from normal SHRIMP practice to achieve rapid acquisition of data at the expense of some measurement precision. Fifty nine detrital grains were measured after random sampling.

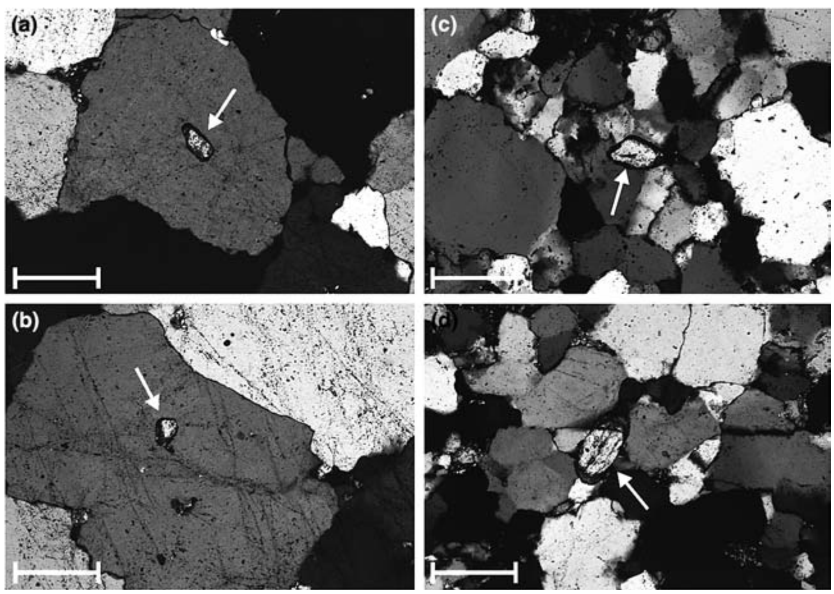

Fig. 2 Photomicrographs with cross-polarizer of **a**,**b** a quartzite (sample 99-38) from the Unterer Lobenklee locality of the Eckergneiss Complex and **c**, **d** of an Acker–Bruchberg quartzite from the Ilsetal. Note that the detrital zircon crystals (marked by *white arrows*) in the Ecker quartzite are enclosed in the quartz grains, whereas, they are located along interstitial sites in the Acker–Bruchberg sample. *Scale bars* denote 500 μm

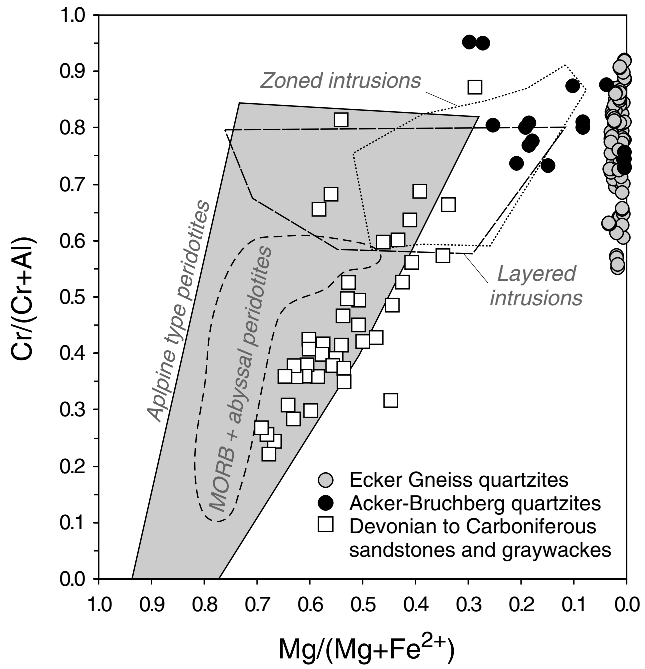

Fig. 3 Diagram Cr/(Cr + Al) versus Mg/(Mg + Fe^{2+}) showing the unique chemical composition of detrital chrome spinels from the Eckergneiss quartzites (data from Martin-Gombojav), when compared to the composition of detrital chromites from Devonian to Carboniferous clastic strata of the Harz Mountains (data from Ganssloser 1999; own unpublished data). Fields for chrome spinels from different geodynamic settings are from Irvine (1967) and Dick and Bullen (1984)

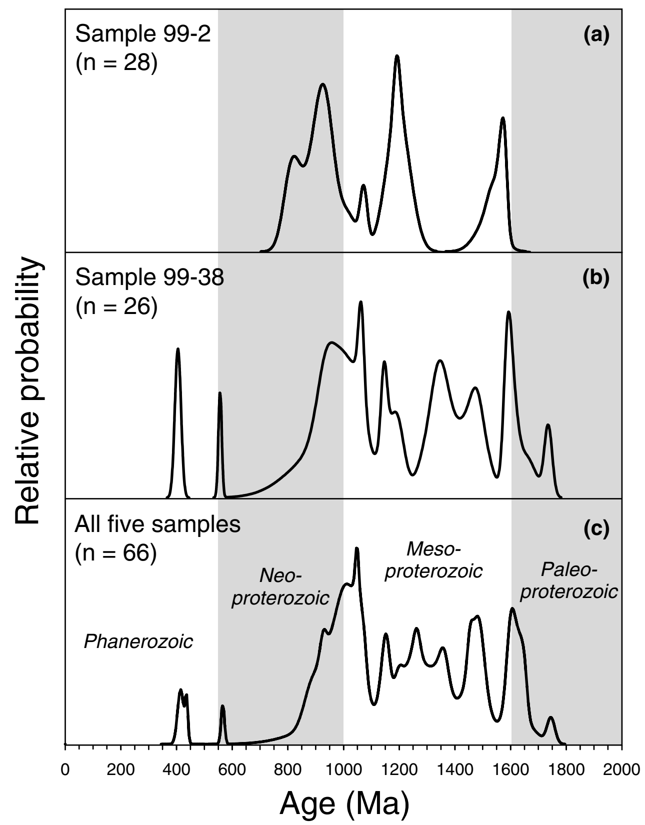

Fig. 4 Cumulative probability curves of concordant SHRIMP ages (see Appendix; Ludwig 1998) from detrital zircons of **a** sample 99-20, **b** sample 99-38, and **c** of all five samples from the Eckergneiss Complex. Age boundaries are according to Gradstein et al. (2004)

The measurements on alteration or recrystallization rims (Fig. 5), however, were preselected and were acquired using the normal SHRIMP procedure. This was done because we initially hoped to be able to date the metamorphism of the EGC by analyzing these zones.

In order to obtain a best age estimate, the Concordia age calculation procedure of Ludwig (1998) was applied, which is based on the two U–Pb isotope ratios and their correlation. Only those data with U–Pb ages that overlap the Concordia with their 2σ error ellipse were used to construct the probability plot shown in Fig. 4. However, in those cases, where we obtained more than a single discordant measurement on a single grain, we used the upper or, in one case, the lower discordia intercept age (see Appendix). Ages and errors were calculated using the Isoplot software of Ludwig (2001). All reported errors represent the 1σ a priori error. Decay constants used are those recommended by IUGS (Steiger and Jäger 1977). The new timescale of Gradstein et al. (2004) was consistently applied throughout the text.

Results

In Fig. 4, we have plotted the cumulative probability plots for two quartzite samples from different localities and for all data. It is evident from all three probability plots that the age population is strongly dominated by Proterozoic ages, ranging from about 900 Ma to about 1800 Ma. The limited amount of data collected from zircon crystals of the individual samples (Fig. 4a, b), however, does not allow us to interpret the differences seen in the fine structure of the Proterozoic age population. Archean age components were not found in any of the samples. An unexpected result is that three zircon crystals from two quartzite localities (samples 99-38 and 0-12) yielded statistically indistinguishable Lower Devonian and Silurian ages of 410 ± 10, 419 ± 10, and 436 ± 5 Ma (Appendix). A single grain with an age of 566 ± 6 Ma was also found in sample 99-38. It should also be noted that we have conducted two SHRIMP analyses (core–rim) on each of these grains, yielding ages that are also statistically indistinguishable from each other (Appendix).

Representative cathodoluminescence (CL) images of the investigated detrital zircon crystals are shown in Fig. 5. Based on the internal growth structure, visualized by the CL images, the zircon population may be roughly divided into the following groups: (1) zircon grains with simple oscillatory growth zones (Fig. 5a–c), (2) zircon crystals with bright-CL zones penetrating into older zircon cores (Fig.5d, f), (3) grains with newly grown rims (Fig. 5i), (4) sector-zoned zircon crystals (Fig. 5g), (5) unusual zircon grains showing curved internal structures

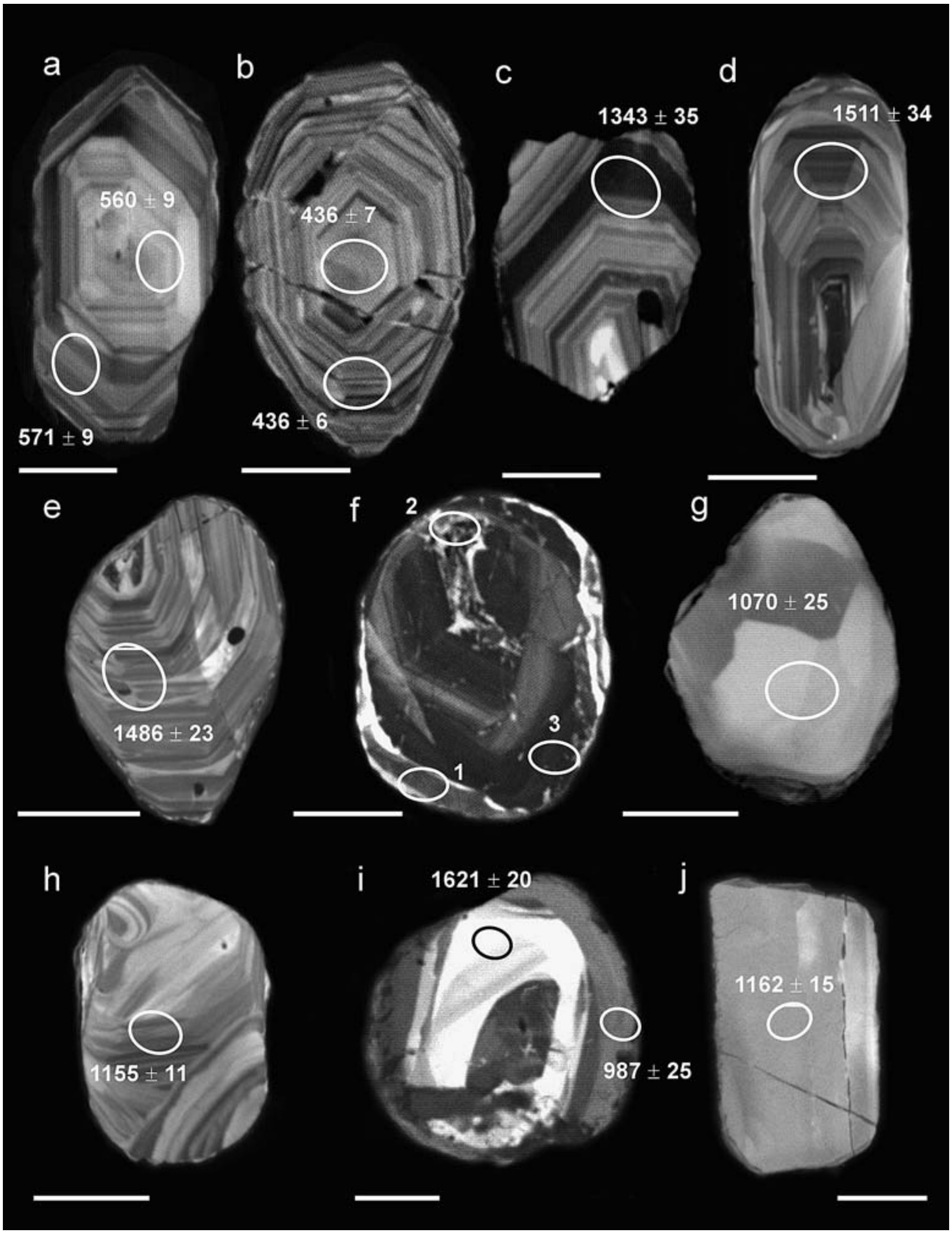

Fig. 5 a–j Cathodoluminescence images of representative detrital zircon crystals from the Eckergneiss Complex. SHRIMP spot localities are marked by *ellipses*. The corresponding $^{206}Pb/^{238}U$ age is also given. SHRIMP data points 1, 2, and 3 shown in **f** are discussed in the text

(Fig. 5h), and (6) relatively homogeneous zircon grains (Fig. 5j). However, we should note that some grains are even more complex and, when considering the internal structure, represent rather mixtures of these groups.

First, we note that the Lower Devonian and Silurian crystals are elongated and exhibit simple oscillatory zoning (Fig. 5a, b). These features clearly point to a magmatic origin. Crystals grown during high-grade metamorphic events are usually multi-facetted with an oval shape (e.g., Grauert and Wagner 1975; Kröner et al. 1994). The occurrence of complex internal structures of older zircon crystals, such as those shown in Fig. 5f – j, indicates that these grains underwent a metamorphic imprint involving fluids (e.g., Geisler et al. 2001, 2003a, 2003b, 2003c; Schaltegger et al. 1999; Tomaschek et al. 2003; Vavra et al. 1996, 1999). We note that inwards penetrating recrystallization zones characterized by a bright CL intensity have been produced by hydrothermal treatment of partially metamict zircon samples at temperatures as low as 175°C (Geisler et al. 2001, 2002, 2003a, 2003b, 2003c). In old zircons, bright-CL zones are mainly characterized by a lesser degree of self-irradiation damage or a higher degree of recrystallization, respectively (unpublished Raman spectroscopic data; see also Geisler5h, have recently been observed after treating an almost fully metamict zircon in hydrothermal solutions (Geisler et al. 2004).

As mentioned in the previous section, we originally hoped that some of these complex zircon crystals would yield ages that could be correlated with the inferred metamorphic evolution of the EGC. However, during the course of the work, it became evident that most of these zircon crystals yield Sveconorwegian (Grenvillian) ages, ranging from ca. 980 to 1,200 Ma (Fig. 4), clearly revealing that the ages reflect metamorphic events in the zircon source region rather than in the EGC. Grains outside this age range usually exhibit simple oscillatory zoning typical for magmatic zircon (Fig. 5c–e). Only three analyses of fluid-induced alteration rims around zircon Z12 (Fig. 5f) yielded ages younger than 900 Ma (see analyses Z12-1/2/3 in Appendix). Although the 2σ error ellipses of these analyses overlap or nearly overlap with the Concordia, significant higher ^{207}Pb/^{206}Pb ages clearly indicate that the data points are discordant. The three analyses fall on a reference line between an upper and lower Concordia age of about 960 and 440 Ma, respectively.

Discussion

Time of sedimentation of the Eckergneiss detritus

As a guide to the following discussion, we have schematically summarized the available and reliable geochronological data of the EGC and correlated these data with the known tectono-stratigraphy of the EGC and of the Harz Mountains (Fig. 6). The inferred tectono-metamorphic history of the EGC, derived from such a picture, is also shown. The most important and decisive observation of the present study is the occurrence of detrital zircon crystals of magmatic origin and of Lower Devonian and Silurian age. This observation has several consequences. It implies that sedimentation of the detritus, now incorporated in the EGC, and the high-grade metamorphism must have taken place after 410 ± 10 Ma, as given by the youngest detrital zircon. The lower limit for high-grade metamorphism is constrained by the intrusion of the Harzburg gabbronorite and the Brocken granite at ~295 Ma, which affected the EGC thermally as shown by mineral reactions (Franz et al. 1997) and an isotopically resetted sphene U–Pb age of 296 Ma (Baumann et al. 1991). It follows that any Cadomian metamorphism in the EGC can unambiguously be excluded. The sedimentation of the EGC protolith thus occurred contemporaneously with the deposition of Devonian to Carboniferous siliciclastic sediments, which make up by far the largest portion of the Palaeozoic outcrop area in the Harz Mountains (Fig. 6). The implications of this paradox, as it might seem, are discussed in below.

Provenance of the Eckergneiss protolith

The EGC metasediments are a suite of Ca- and alkali-poor metapelites and metapsammites of high compositional maturity. This composition reflects, together with a refractory heavy mineral assemblage of mainly zircon, chrome spinel, rutile, and occasional garnet as major detrital heavy minerals, a passive continental margin provenance (Martin-Gombojav 2003, unpublished doctoral thesis). It is similar to the major Rhenohercynian lithologies, which can be attributed to a passive continental margin setting at the southern rim of the Old Red Sandstone Continent (Franke 2001). As discussed in the previous section, the EGC protolith's sedimentary sequence must have been deposited between the Lower Devonian and Upper Carboniferous. Taking into account the currently inferred palaeogeographic reconstructions of relevant terranes for this time span (e.g., Torsvik 1998; Pharaoh 1999; Robardet 2003) and the position of the EGC within the Rhenohercynian domain, a number of potential source areas of the detritus

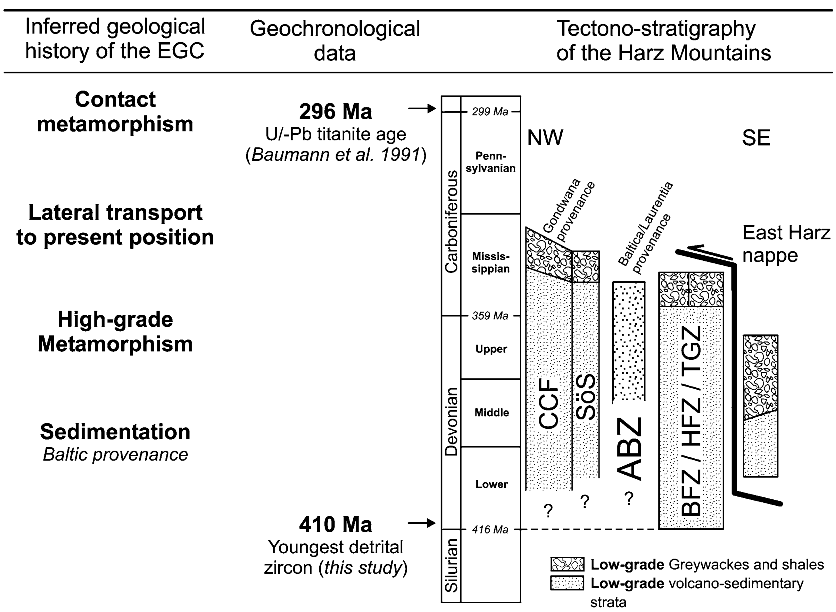

Fig. 6 Schematic summary of geochronological data and the inferred geological history of the Eckergneiss Complex in comparison with the tectono-stratigraphy of the Harz Mountains (modified after Ganssloser (1999), using data of Mohr (1978); Wachendorf (1986); provenance data are from Haverkamp et al. (1992) and Huckriede et al. (1998)). Age boundaries between series epochs are from Gradstein et al. (2004). For abbreviations see Fig. 1

of the Eckergneiss protolith have to be considered. In early Devonian time Baltica—the Avalonia microplate with Gondwana affinity—and Laurentia had already been amalgamated in the course of the Caledonian orogeny, now forming Laurussia, i.e., the so called Old Red Continent. At that time, Laurussia was located to the north of the Rhenohercynian Ocean, which was subsequently closed by the northward motion of the Gondwana Supercontinent. The collision of Gondwana with the Old Red Continent in Carboniferous times is recorded by the Variscian orogeny in Central Europe. The clastic strata of the Rhenohercynian domain are characterized in temporal succession by material shed from the active continental margin of the Variscan front in the southeast, i.e., from peri-Gondwana/Gondwana terranes, and by detritus derived from the Old Red continent to the northwest (Haverkamp et al. 1992; Huckriede et al. 1998). Haverkamp et al. (1992) discovered that detrital zircons in Rhenohercynian Lower Devonian sandstones show U–Pb systematics, which hint towards an ultimate derivation from various Scandinavian sources, including south Greenland and the Caledonides on both sides of the Iapetus suture. They consider an origin from "positive" areas within the "Mid-European Caledonides", i.e., the Danish–North German–Polish Caledonides according to present terminology. A change towards a major contribution of detrital zircons with a Gondwana age provenance is documented by Lower Carboniferous deposits (Haverkamp et al. 1992).

The Gondwana and peri-Gondwana terranes in North Africa, including the Saharan Metacraton (Abdelsalam et al. 2002), North America, and Europe are characterized by volcanism and plutonism between about 510 Ma and 900 Ma ago (e.g., Abdelsalam et al. 2002; Boullier 1991; Bregar et al. 2002; Cahen et al. 1984; Franke 2000; Ingle at al. 2003; Pin 1991; Rocci et al. 1991; Fig. 7e). Cambrian ages were also reported from Cadomian terranes (e.g., Zulauf et al. 1997; Dörr et al. 2002). Tichomirowa et al. (2000) accentuated the absence of Grenvillian ages in detrital zircon populations in various gneisses of the Erzgebirge within the Saxothuringian domain, which exhibits a Gondwana affinity. The authors detected zircon age groups of about

Fig. 7 Comparison of the cumulative probability curve (Ludwig 1998) of SHRIMP ages from detrital zircons of the Eckergneiss Complex with those obtained from age data of magmatic and metamorphic rocks from various potential source areas of **a–d** the southern Baltic Shield and **e** North Africa (Gondwana). The inset map shows the lithotectonic domains of SW Scandinavia (after Söderlund et al. 1999, and references therein): *SF* Svecofennian domain, *TIB* Transscandinavian Igneous Belt, *ES* Eastern Segment, *SFDZ* Sveconorwegian Frontal Deformation Zone, *WS* Western Segment, *O* Oslo area, *K* Kongsberg sector, *B* Bamble sector, *T* Telemark sector, *R–A* Rogalan Agder sector. Data sources: (a) compilation by Å häll and Larson (2000); (b) compilation and references in Söderlund et al. (1999); (c) compilation and references in Åhäll and Larson (2000), metamorphic zircon data are from a compilation of Söderlund et al. (2002); (d) compilation of Bingen et al. (2003), metamorphic zircon data from the R–A sector are from Möller et al. 2002; (e) compilation of Boullier (1991), Cahen et al. (1984), and of Rocci et al. (1991), and Bregar et al. (2002)

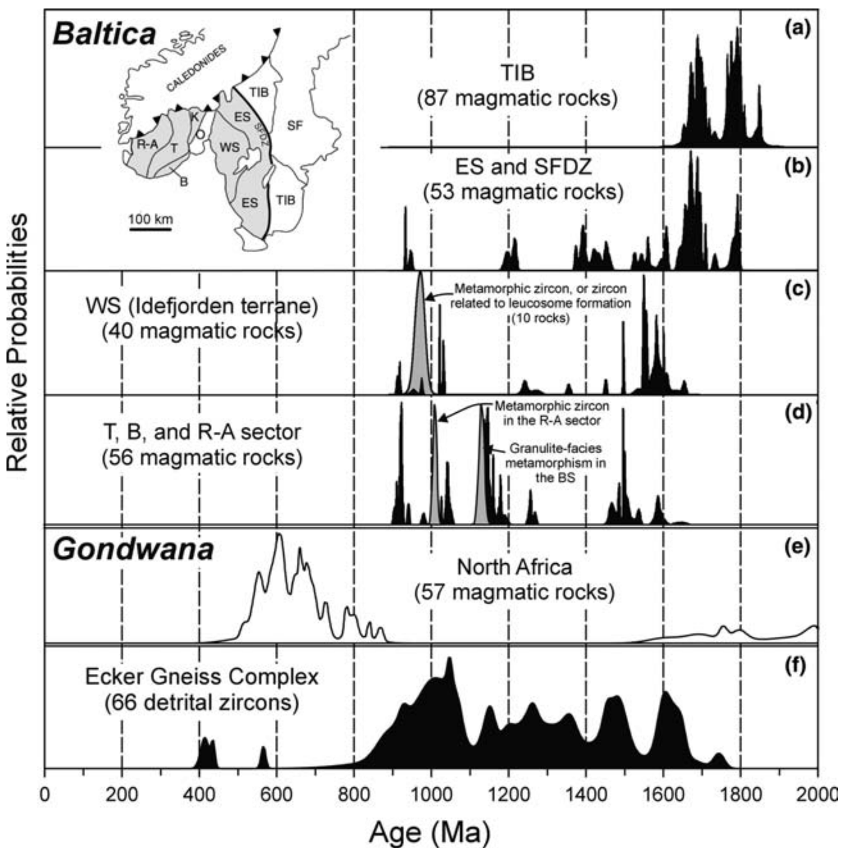

575 Ma, 600–700 Ma, 2.1–2.2 and 2.7–2.8 Ga, suggesting a derivation from the West African Craton.

The North African cratons are dominated by ~2.0 Ga old gneisses and additionally contain Neo-Proterozoic and Archean rocks. Neo-Proterozoic and Archean ages are also known from Greenland, North America (e.g., Nutman et al. 1996; Bevier et al. 1990; Zhao et al. 2002), and the Amazonian craton (Tassinari and Macambira 1999) and are commonly found in provenance studies involving sediments derived from Laurentian (e.g., Karabinos and Gromet 1993; Dickinson and Gehrels 2003; Strachan et al. 1995) and Gonwanan sources (e.g., Fernández-Suárez et al. 2002; Zeh et al. 2001). The strong dominance of Meso-Proterozoic age components in the detrital zircon population of the EGC without a significant Neo-Proterozoic or Archean contributions[2] (Fig. 4) along with the fact that only one single zircon yielded an age of 566 ± 6 Ma (Fig. 5a) precludes a major derivation of the detritus from Laurentia, Amazonia, Gondwana, and peri-Gondwana. This reasoning applies also to the question of an involvement of the MGCR as a possible detritus source. Zeh et al. (2001) found distinctively Gondwana zircon age characteristics in rocks of the MGCR with the Avalonian–Cadomian orogenic belt and the West African and/or eastern Amazonian cratons as equally dominant sources and an only minor (10%) contribution from the Grenvillian belt. The latter would have to be translated into "Sveconorwegian belt" for its European (Baltica) continuation.

The absence of a significant Archean sediment contribution (< 8%)[3] in the EGC is also in agreement with the conventional U–Pb data of detrital zircon fractions, which point to an upper Concordia intercept of about 1,600 Ma (Baumann et al. 1991). Instead, the observed distribution of Proterozoic ages is entirely consistent with an origin of the detritus from a SW Baltic source (Fig. 7). The SW Baltic provenance becomes evident when comparing the observed age spectrum with the geochronology of different lithotectonic domains within the Baltic Shield (inset map of Fig. 7, see also Nironen 1997; Gaál and Gorbatschev 1987). It is evident from Fig. 7 that the observed Proterozoic age spectrum matches best with the magmatic and metamorphic evolution of the western segment of south Sweden and the Sveoconorwegian domains in south Norway (e.g., Bingen et al. 2003 and references therein). Furthermore, the ages of metamorphic growth zones (Fig. 5i), sector-zoned zircon (Fig. 5g), and recrystallized zircon (Fig. 5h, j; see also Geisler et al. 2004) fall well in the age intervals of 1,120–1,150 Ma and 960–1,030 Ma, which have been determined for early and late Sveconorwegian granulite-facies metamorphism in these areas, respectively (e.g., Bingen et al. 2003; Möller et al. 2002).

[2] Note that we have obtained 66 concordant ages, which means that we can state with a 95% certainty that a possible Archean component must be smaller that 8% (see Vermeesch 2004).

[3] See footnote 2.

Whereas tracing the source of the Meso-Proterozoic zircon crystals is relatively straightforward, the origin of the Silurian or Caledonian component is more of a problem. Caledonian ages are known from those parts of Laurentia and Baltica (e.g., Scotland and north Norway) that were affected by the Caledonian orogeny (e.g., Gee and Sturt 1985), but also from various localities within the Mid-European Variscides (e.g., Anthes and Reischmann 2001; Franke 2001, and references therein). However, the strong SW Baltic provenance of the detritus suggests that the Caledonian zircons of the EGC were derived either from the Caledonian nappes in southern Scandinavia or, more likely, from the geographically closer Danish-North German–Polish Caledonides. One may speculate that one of these Caledonic areas is also a potential source for the unique detrital chrome spinel fraction (Fig. 3). However, a problem is posed by the fact that to the best of our knowledge no significant chromite source is known in the exposed part of the southern and central Baltic Shield as well as in the still existing portions of the severely eroded south Scandinavian Caledonian nappes. The Danish-North German–Polish Caledonides rest deeply subsided under thick post-Silurian sediments and the same applies to the southwestern extension of the Baltic Shield beneath most of Denmark where the Sveconorwegian orogenic belt continues as far west as into the Danish North Sea (Obst et al. 2004). It can thus, likewise, be speculated that a structural high of the concealed Sveconorwegian domain, which was exposed to erosion during the Devonian and/or Carboniferous, might be the missing detritus source for chromites as well as for zircons.

Mode of emplacement and origin of the Eckergneiss allochthon: potential implications for the Variscan geodynamics

Since sedimentation in the Rhenohercynian and in the EGC-protolith was virtually synchronous, the high-grade EGC can hardly be seen as an uplifted segment of the Avalonian basement of the Rhenohercynian domain from beneath the present position of the EGC, as was suggested by Franz et al. (1997). A possible scenario being able to accommodate the reported new age data and other observations together with longer known facts would be that the EGC is a remnant of a tectonic nappe. The root zone of this nappe must be deep-seated enough to allow for the intense and partially dynamic metamorphism.

It would be tempting to search the root zone of the EGC outside the Rhenohercynian domain, where high-grade metamorphic entities are known (e.g., Reinhardt and Kleemann 1994; Willner et al. 2000). Constraining facts for the location of a possible root are: the lateral transport must have taken place prior to ~295 Ma and, more crucial, the sediment supply of the protolith must have partially involved the same sources as certain

Rhenohercynian clastic sediments. This reasoning focuses around the question of zircon age spectra and chrome spinel characteristics. Devonian through earliest Carboniferous sediments outside, but also inside (e.g., Harz greywackes, Fig. 6), the Rhenohercynian zone were derived from Cadomian basement to the southeast, i.e., yielded Gondwana age spectra from detrital minerals (Haverkamp et al. 1992; Huckriede et al. 1998). Gondwana zircon age spectra are also reported from the MGCR (Zeh et al. 2001). On the other hand, Baltic provenances are known from certain Lower Devonian to Upper Carboniferous sandstones exposed in the Rhenish Massif and the Harz Mountains (e.g., the ABQ, Fig. 6), in the Carboniferous of the Pennine Basin, and in Carboniferous sandstones of the North Sea (Hallsworth et al. 2000; Haverkamp et al. 1992; Huckriede et al. 1998; Morton et al. 2001). Based on the observed Baltic provenance of the EGC protolith, it follows that the root zone of the EGC cannot be situated too far away from the Old Red continent to the north, i.e., is possibly located inside the Rhenohercynian domain. This hypothesis, which seems to be a paradox at first glance, is supported by the co-occurrence of unusual low-Mg chrome spinels together with a majority of Mg-rich chrome spinels in the clearly Rhenohercynian Lower Carboniferous ABQ. The parallel occurrence of low-Mg chrome spinels, which are the only type of chromite in the EGC (Fig. 3), but a minor component in the ABQ, suggests involvement of an identical though not exclusive source of the detritus of both units and furthermore precludes postdeposition Mg-loss within the EGC.

Within the Harz Mountains and surrounding areas there is no counterpart of the metamorphic EGC lithology and thus no obvious straightforward candidate for a possible root zone. As the entire eastern Harz is a succession of allochtonous units, which were transported as tectonic nappes from the east or southeast (e.g., Franke 2001), the EGC would fit into this general scenario. Its geographical position is within the limits of the Harz allochthonous complex, as shown in Fig. 3 of Franke (2001). The northwestern front of the allochthon is marked by the ABQ. The most likely candidate for a suture, which might be an expression of the EGCs' root zone, is situated between the MGCR and the Northern Phyllite Zone, which were regarded by Franke (2001) as root of the allochthonous units in the Rhenohercynian Belt. The EGC would in this case barely be just another segment of the stacked allochthon of the eastern and southern Harz Mountains. In a written personal communication, of December 2002, W. Franke classified the EGC as an allochthonous wedge at the base of the Giessen/Harz Nappe.

A remaining problem may be the position of the EGC wedged in between the Brocken Granite to the east and the Harzburg Gabbronorite to the west. The intrusions are certainly autochthonous and related to the Oker Granite intrusion farther west in the parautochthon of the Harz Mountains. This position gave rise to the former view of the EGC being passively lifted into the present position by ascending magma. We suggest that the location of the EGC within the major plutonic complexes of the Harz Mountains is not accidental, but possibly either due to forceful or gravitational subsidence into the igneous complex or as part thereof. Contrary to this model, the present position of the EGC is connected with a thrust plane, which was merely used by magma for the uppermost portion of its ascent. The geometry of the Brocken intrusion could reflect a tectonic imprint of southeastward dipping fault or thrust planes by overlapping the EGC from the southeast with a gently southeastward inclining interface with the EGC (Wachendorf 1986).

The problem of the possible paradox of a Rhenohercynian affinity of the protolith's sedimentary character, including the zircon and chromite provenances of the EGC in connection with a "non-Rhenohercynian" metamorphic grade, can be solved with respect to the allochthonous nature of the EGC. It can be both Rhenohercynian and medium- to high-grade metamorphic. A possible scenario can be drawn from a geodynamic model developed by Oncken (1997). According to Oncken (1997), the MGCR southeast of the Rhenohercynian (Fig. 1a) is essentially composed of a Lower Carboniferous magmatic arc association, resting on a stack of medium pressure–medium temperature rocks of inferred Rhenohercynian origin. This implies that medium-grade metamorphic rocks of Rhenohercynian provenance exist east of the Harz Mountains concealed beneath the MGCR and, according to Oncken (1997), even still farther east under the Saxothuringian Zone. The author suggested that in the progress of collisional tectonics, the Rhenohercynian passive margin sequence was first underthrust below the upper plate wedge to the east and later accreted under formation of imbricate fans. In line with this scenario, the EGC would be an upthrusted wedge of the concealed eastern extension of the Rhenohercynian, which became incorporated in the nappe movement to the northwest together with the other units of the Rhenohercynian allochthon of the Harz Mountains. According to this mechanism, the EGC would be a klippen-like segment of the southeastern Rhenohercynian that is derived from a relatively deep level of the underthrust Rhenohercynian. The interpretation of the EGC as part of a nappe would demand a slab-like geometry. Indeed, such geometry is indicated by geophysical investigations of Düweke et al. (1976), which figured the maximum thickness of the EGC with ca. 400 m. The high-grade granulite-facies overprinting could then be due to the mainly static influence of the magmatic arc of the MGCR, as suggested by W. Franke in a written communication of December 2002. Nevertheless, new petrographic observations (Martin-Gombojav 2003, unpublished doctoral thesis; see also Sect. 2) and P–T estimates on kinzingites (Schlüter 1983, unpublished doctoral thesis) indicate that the metamorphism in the Eckergneiss occurred at rather low pressures and under progressively higher temperatures up to granulite-facies conditions, which does not fit into a typical P–T scenario expected in a subduction environment.

Before ending the discussion, we should mention that an alternative mode of emplacement of the EGC has to be considered that is based on a concept of strike-slip movements of Variscan terranes of different P–T–t histories, which occurred between about 360 Ma and 320 Ma, as proposed by Krohe (1996). In contrast to the common view that the fault-bounded crustal blocks in the Variscan belt are the result of the amalgamation of continental microplates in the course of the Variscan orogeny (e.g., Franke 1989), which the above model is based on, Krohe (1996) suggested that the fault-bounded entities were created by intraplate deformation of a weak domain of continental lithosphere, which occurs significantly after accretion. In such a tectonic picture, the EGC would represent a fault-bounded complex with an origin, which must be located far east or south east of the present location. We note here that strike-slip displacements can reach distances larger than 500 km (e.g., Tapponier et al. 1990).

Both models would afford metamorphism of both types before commencement of tectonic movement, very likely in short temporal succession and in the described order. However, a problem might be posed by the good preservation of many orthopyroxenes and cordierite in the investigated granulite-facies rocks, which must have been incorporated in the transport. On the other hand, these movements might explain that a minority of the blocky orthopyroxenes of granulite-facies parageneses are tectonically bent.

It is obvious that a detailed knowledge about the timing and the conditions of the metamorphism of the EGC may help to locate the root zone of the EGC, which, in turn, would be another important piece of knowledge needed to understand the complex kinematic pattern of the Variscan Belt. Detailed geochronological and further petrological work is thus envisaged for the next future. For the time being, the location of the root zone remains a matter of speculation.

Acknowledgements Dr. W. Wegener (Nationalpark Hochharz) and K. Surkau (Nationalpark Harz) are kindly acknowledged for permitting us to take rock samples from the EGC area. J. Richards, B. Stütze, and E. Thun are thanked for mineral separation. We would also like to thank J. Schlüter for leaving samples at our disposal and for many fruitful discussions. Critical comments on an earlier draft of the manuscript by A. Krohe and very constructive reviews of G. Zulauf and an anonymous reviewer are appreciated. We are also grateful to the Deutsche Forschungsgemeinschaft (project VI 88/2-1 to RV and TG) and the Deutsche Akademische Austauschdienst (scholarship no. A/99/07919 to NMG) for their financial support.

Appendix

SHRIMP data of detrital zircon grains from five quartzite samples of the EGC

Spot	U (ppm)	Th (ppm)	Pb (ppm)	$^{204}Pb/^{206}Pb$	$^{207}Pb/^{206}Pb$	±1σ	$^{208}Pb/^{232}Th$	±1σ	$^{207}Pb/^{235}U$	±1σ	$^{206}Pb/^{238}U$	±1σ	$^{206}Pb/^{238}U$ age (Ma)	±1σ	$^{207}Pb/^{235}U$ age (Ma)	±1σ	$^{207}Pb/^{206}Pb$ age (Ma)	±1σ	$^{208}Pb/^{232}Th$ age (Ma)	±1σ	Best age estimate[a] (Ma)	±1σ
Sample 99-38																						
Z1-1	128	86	46	0.00011	0.1057	0.0009	0.0904	0.0017	4.691	0.087	0.3220	0.0050	1,799	24	1,766	16	1726	16	1,750	32	**1,745**	**14**
Z1-2	166	62	62	0.00017	0.1083	0.0009	0.1031	0.0022	5.322	0.096	0.3563	0.0054	1,964	26	1,872	15	1,772	14	1,983	40	–	–
Z12-1	825	43	71	0.00058	0.0618	0.0014	0.0324	0.0052	0.758	0.032	0.0889	0.0030	549	18	573	19	668	47	644	101	*961*	*55*
Z12-2	1017	86	118	0.00079	0.0675	0.0012	0.0266	0.0038	1.105	0.044	0.1188	0.0040	723	23	756	21	853	38	530	75	–	–
Z12-3	1,196	339	135	0.00109	0.0637	0.0014	0.0317	0.0016	0.944	0.040	0.1075	0.0036	658	21	675	21	732	47	631	31	–	–
Z14-1	202	78	31	0.00192	0.0696	0.0039	0.0394	0.0034	1.298	0.090	0.1353	0.0046	818	26	845	40	916	116	780	67	–	–
Z15-1	103	85	11	0.00022	0.0591	0.0027	0.0285	0.0009	0.740	0.038	0.0908	0.0015	560	9	563	22	571	100	568	17	**566**	**6**
Z15-2	216	153	22	0.00014	0.0584	0.0013	0.0288	0.0006	0.746	0.021	0.0926	0.0014	571	8	566	12	545	48	574	12	–	–
Z16-1	92	62	19	0.00013	0.0894	0.0017	0.0568	0.0014	2.294	0.060	0.1861	0.0030	1,100	16	1,210	19	1,413	36	1,117	27	–	–
Z18-1	652	256	188	0.00028	0.0988	0.0008	0.0724	0.0027	3.732	0.132	0.2739	0.0091	1560	46	1,578	28	1,602	15	1,413	50	**1,599**	**14**
Z18-2	350	156	91	0.00031	0.0983	0.0011	0.0695	0.0027	3.296	0.121	0.2432	0.0082	1,403	42	1,480	29	1,592	21	1,358	51	–	–
Z20-1	204	122	61	0.00117	0.0954	0.0023	0.0683	0.0032	3.408	0.149	0.2590	0.0088	1,485	45	1,506	34	1,536	45	1,335	61	**1,511**	**34**
Z2-1	728	268	132	0.00006	0.0755	0.0004	0.0519	0.0009	1.857	0.031	0.1784	0.0026	1,058	14	1,066	11	1,081	11	1,022	17	**1,073**	**10**
Z21-1	195	122	16	0.00236	0.0563	0.0063	0.0204	0.0018	0.527	0.064	0.0680	0.0024	424	14	430	42	463	249	409	35	**419**	**10**
Z21-2	192	120	15	0.00063	0.0616	0.0042	0.0223	0.0013	0.567	0.046	0.0668	0.0023	417	14	456	30	660	148	446	26	–	–
Z25-1	1,079	1,038	270	0.00000	0.0829	0.0002	0.0628	0.0009	2.428	0.037	0.2124	0.0031	1,242	17	1,251	11	1,267	6	1,230	18	**1,267**	**6**
Z26-1	248	170	21	0.00354	0.0439	0.0066	0.0179	0.0016	0.391	0.062	0.0646	0.0023	404	14	335	45	0	28	360	31	**410**	**10**
Z26-2	242	164	19	0.00182	0.0465	0.0051	0.0185	0.0014	0.428	0.051	0.0667	0.0023	416	14	362	36	37	234	371	27	–	–
Z28-1	109	84	35	0.00050	0.1093	0.0028	0.0815	0.0037	4.051	0.185	0.2687	0.0094	1,534	48	1,644	37	1,788	46	1,584	69	–	–

Spot	U (ppm)	Th (ppm)	Pb (ppm)	$^{204}Pb/^{206}Pb$	$^{207}Pb/^{206}Pb$	±1σ	$^{208}Pb/^{232}Th$	±1σ	$^{207}Pb/^{235}U$	±1σ	$^{206}Pb/^{238}U$	±1σ	$^{206}Pb/^{238}U$ age (Ma)	±1σ	$^{207}Pb/^{235}U$ age (Ma)	±1σ	$^{207}Pb/^{206}Pb$ age (Ma)	±1σ	$^{208}Pb/^{232}Th$ age (Ma)	±1σ	Best age estimate[a] (Ma)	±1σ
Z29-1	204	143	53	0.00115	0.0859	0.0025	0.0632	0.0029	2.646	0.126	0.2233	0.0076	1,299	40	1,314	35	1,337	57	1,238	55	**1,311**	**35**
Z30-1	395	210	127	0.00036	0.0996	0.0009	0.0856	0.0031	4.025	0.144	0.2931	0.0098	1,657	49	1,639	29	1,616	17	1,661	58	**1,620**	**17**
Z31-1	274	155	76	0.00075	0.0918	0.0016	0.0664	0.0028	3.126	0.125	0.2471	0.0083	1,423	43	1,439	31	1462	33	1,299	52	**1,448**	**28**
Z32-1	24	19	7	0.00761	0.0943	0.0227	0.0631	0.0113	2.088	0.525	0.1607	0.0077	961	42	1,145	174	1,513	469	1,236	214	**956**	**42**
Z34-1	1,195	430	127	0.00054	0.0691	0.0012	0.0309	0.0013	0.966	0.038	0.1014	0.0034	623	20	686	20	902	35	616	25	–	–
Z34-2	1,076	373	164	0.00025	0.0725	0.0008	0.0455	0.0017	1.484	0.054	0.1485	0.0049	892	28	924	22	1,000	23	898	33	–	–
Z35-1	113	66	24	0.00261	0.0728	0.0052	0.0502	0.0040	1.713	0.143	0.1708	0.0060	1,016	33	1,014	54	1,007	146	991	77	**1,016**	**33**
Z36-1	160	139	34	0.00347	0.0678	0.0065	0.0428	0.0031	1.481	0.156	0.1583	0.0055	947	31	923	64	863	198	847	61	**947**	**31**
Z37-1	350	143	102	0.00001	0.1048	0.0006	0.0880	0.0031	3.946	0.137	0.2731	0.0091	1556	46	1,623	28	1,711	11	1,704	57	–	–
Z38-1	31	32	12	0.01463	0.0469	0.0295	0.0445	0.0117	1.116	0.711	0.1726	0.0085	1,027	47	761	355	49	1,055	879	226	**1,028**	**47**
Z39-1	430	96	101	0.00097	0.0878	0.0014	0.0659	0.0039	2.710	0.106	0.2238	0.0075	1,302	39	1,331	29	1,379	32	1,289	73	**1,350**	**26**
Z40-1	236	64	66	0.00125	0.0836	0.0022	0.0787	0.0053	2.972	0.134	0.2580	0.0087	1,480	45	1,401	34	1,282	51	1,530	100	**1,391**	**35**
Z4-1	363	213	103	0.00061	0.0933	0.0012	0.0708	0.0027	3.258	0.122	0.2532	0.0085	1,455	44	1,471	29	1,494	25	1,382	51	**1,486**	**23**
Z41-1	216	111	58	0.00169	0.0889	0.0027	0.0623	0.0035	2.862	0.139	0.2336	0.0079	1,353	41	1,372	36	1,402	59	1,222	67	**1,368**	**36**
Z42-1	163	75	37	0.00149	0.0749	0.0032	0.0588	0.0038	2.089	0.120	0.2023	0.0069	1,188	37	1,145	40	1,066	85	1,154	72	**1,169**	**35**
Z43-1	160	89	52	0.00131	0.1080	0.0030	0.0839	0.0045	4.142	0.194	0.2782	0.0095	1,582	48	1,663	38	1,766	51	1,629	84	**1,661**	**38**
Z45-1	605	103	165	0.00032	0.0988	0.0008	0.0482	0.0029	3.759	0.132	0.2761	0.0092	1,572	46	1,584	28	1,601	15	951	56	**1,599**	**14**
Z5-1	346	125	70	0.00003	0.0782	0.0005	0.0609	0.0011	2.121	0.037	0.1966	0.0030	1,157	16	1,156	12	1,153	14	1,195	21	**1,155**	**11**
Z6-1	19	38	5	0.00107	0.0663	0.0105	0.0527	0.0029	1.650	0.270	0.1805	0.0046	1,070	25	989	104	816	336	1,038	56	**1,070**	**25**
Z8-1	471	299	110	0.00052	0.0800	0.0012	0.0615	0.0023	2.292	0.088	0.2078	0.0069	1,217	37	1,210	27	1,197	30	1,206	43	**1,205**	**25**
Sample 0-40																						
Z10-1	1,276	417	225	0.00002	0.0743	0.0002	0.0531	0.0008	1.786	0.028	0.1743	0.0026	1,036	14	1,040	10	1,050	7	1,046	16	**1,048**	**6**
Z1-1	213	89	39	0.00018	0.0694	0.0009	0.0497	0.0011	1.684	0.035	0.1759	0.0027	1,045	15	1,002	13	911	26	979	22	**1,045**	**15**
Z11-1	160	93	34	0.00642	0.0727	0.0051	0.0147	0.0031	1.525	0.114	0.1520	0.0025	912	14	940	46	1,007	144	295	61	*1,089*	*49*[b]
Z11-2	3,477	371	377	0.00062	0.0758	0.0004	0.0271	0.0009	1.153	0.018	0.1103	0.0016	675	9	779	9	1,089	10	541	18	–	–
Z14-1	876	204	162	0.00014	0.0789	0.0004	0.0561	0.0010	2.014	0.032	0.1852	0.0027	1,095	15	1,120	11	1,169	9	1,104	19	–	–
Z15-1	119	85	27	0.00002	0.0803	0.0011	0.0628	0.0013	2.253	0.050	0.2036	0.0032	1,195	17	1,198	16	1,203	27	1,231	24	**1,197**	**15**
Z17-1	103	21	15	0.00449	0.0765	0.0085	0.0508	0.0105	1.181	0.143	0.1119	0.0041	684	24	792	67	1,108	224	1,001	202	–	–
Z18-1	681	145	115	0.00089	0.0761	0.0012	0.0476	0.0026	1.714	0.066	0.1634	0.0055	976	30	1,014	25	1,097	32	939	50	**1,031**	**24**
Z19-1	535	121	88	-0.00004	0.0854	0.0006	0.0625	0.0022	1.927	0.068	0.1636	0.0055	977	31	1,090	24	1,324	13	1,225	43	–	–
Z2-1	166	24	31	0.00011	0.0809	0.0009	0.0496	0.0024	2.125	0.042	0.1906	0.0029	1,125	16	1,157	14	1,218	21	978	47	–	–
Z3-1	73	42	21	0.00022	0.0923	0.0015	0.0789	0.0021	3.299	0.080	0.2593	0.0042	1,486	22	1,481	19	1,473	31	1,536	39	**1,482**	**19**
Z4-1	402	95	113	0.00129	0.0909	0.0017	0.0776	0.0049	3.281	0.132	0.2618	0.0088	1,499	45	1,476	31	1,444	35	1,510	91	**1,464**	**31**
Z7-1	42	17	13	0.00006	0.0989	0.0020	0.0853	0.0034	3.841	0.107	0.2816	0.0049	1,600	25	1,601	22	1,604	37	1,654	63	**1,601**	**22**
Z8-1	384	21	94	0.00004	0.0912	0.0005	0.0657	0.0040	3.219	0.053	0.2562	0.0038	1,470	20	1,462	13	1,450	10	1,286	76	**1,454**	**10**
Z9-1	61	22	11	0.00019	0.0697	0.0029	0.0516	0.0034	1.701	0.080	0.1769	0.0030	1,050	16	1,009	30	920	86	1,017	65	**1,047**	**16**
Sample 0-12																						
Z1-1	131	50	27	0.00008	0.0756	0.0012	0.0615	0.0017	2.100	0.049	0.2015	0.0032	1,184	17	1,149	16	1,084	31	1,207	33	**1,162**	**15**
Z2-1	312	235	25	0.00034	0.0507	0.0015	0.0220	0.0005	0.489	0.017	0.0700	0.0011	436	7	404	12	227	68	441	10	**436**	**5**
Z2-2	449	290	34	0.00002	0.0555	0.0010	0.0222	0.0004	0.535	0.013	0.0700	0.0011	436	6	435	9	431	40	444	9	–	–
Z3-1	69	29	14	0.00031	0.0731	0.0023	0.0561	0.0026	1.961	0.072	0.1945	0.0032	1,146	17	1,102	25	1,017	62	1,104	50	**1,138**	**17**
Z4-1	27	14	6	0.00048	0.0771	0.0047	0.0611	0.0045	2.263	0.150	0.2129	0.0043	1,244	23	1,201	47	1,124	121	1,199	86	**1,242**	**22**
Z4-2	140	75	36	0.00009	0.0852	0.0010	0.0716	0.0015	2.835	0.057	0.2414	0.0037	1,394	19	1,365	15	1,320	22	1,398	29	**1,361**	**15**
Sample 0-100																						
Z14-1	314	143	51	0.00018	0.0720	0.0009	0.0500	0.0010	1.515	0.031	0.1526	0.0023	915	13	937	13	987	25	986	20	–	–
Z14-2	70	23	21	0.00011	0.0964	0.0017	0.0858	0.0034	3.892	0.099	0.2928	0.0048	1,656	24	1,612	21	1,555	33	1,664	64	**1,621**	**20**
Z15-1	297	99	53	0.00007	0.0751	0.0007	0.0534	0.0011	1.824	0.034	0.1761	0.0027	1046	15	1,054	12	1,071	18	1,051	21	**1,055**	**12**

Z2-1	64	72	21	0.00013	0.0909	0.0016	0.0785	0.0017	3.312	0.083	0.2642	0.0043	1,511	22	1,484	20	1,445	33	1,528	31	**1,491**	**19**
Z3-1	137	60	39	0.00149	0.0927	0.0031	0.0703	0.0047	3.212	0.164	0.2512	0.0086	1,445	44	1,460	39	1,483	64	1,374	89	**1,456**	**39**
Z4-1	387	147	107	0.00083	0.0928	0.0016	0.0719	0.0033	3.278	0.129	0.2561	0.0086	1,470	44	1,476	31	1,484	32	1,404	63	**1,480**	**27**
Z7-1	99	36	20	0.00272	0.0786	0.0056	0.0536	0.0062	1.843	0.155	0.1701	0.0060	1,013	33	1,061	55	1,162	142	1,056	120	**1,015**	**33**
Z8-1	178	35	43	0.00103	0.0862	0.0024	0.0567	0.0065	2.752	0.129	0.2314	0.0079	1,342	41	1,343	35	1,344	54	1,114	125	**1,343**	**35**
Sample 99-20																						
Z1-1	215	86	66	0.00007	0.1007	0.0007	0.0855	0.0017	4.023	0.071	0.2896	0.0044	1,640	22	1,639	14	1,638	13	1,658	31	**1,638**	**12**
Z1-2	244	121	79	0.00007	0.1012	0.0005	0.0886	0.0015	4.159	0.069	0.2981	0.0045	1,682	22	1,666	14	1,646	10	1,716	28	**1,651**	**10**
Z13-1	124	49	25	0.00136	0.0785	0.0036	0.0518	0.0042	1.979	0.121	0.1829	0.0063	1,083	35	1,108	41	1,159	92	1,021	80	**1,088**	**34**
Z14-1	462	141	85	0.00005	0.0791	0.0004	0.0541	0.0010	1.995	0.033	0.1829	0.0027	1,083	15	1,114	11	1,175	11	1,065	19	–	–
Z14-2	445	111	79	0.00002	0.0779	0.0005	0.0584	0.0011	1.912	0.032	0.1780	0.0027	1,056	15	1,085	11	1,144	13	1,147	22	–	–
Z16-1	29	20	8	0.00870	0.0651	0.0195	0.0391	0.0109	1.480	0.455	0.1650	0.0071	985	39	922	188	777	528	776	213	**985**	**39**
Z17-1	115	87	25	0.00265	0.0708	0.0050	0.0474	0.0031	1.662	0.137	0.1703	0.0060	1,014	33	994	52	951	145	935	60	**1,012**	**33**
Z18-1	1,380	415	205	0.00019	0.0825	0.0006	0.0456	0.0016	1.654	0.058	0.1455	0.0048	876	27	991	22	1,256	14	901	31	–	–
Z2-1	85	48	17	0.00303	0.0451	0.0084	0.0299	0.0058	1.034	0.200	0.1663	0.0061	992	34	721	100	0	41	595	113	**977**	**34**
Z21-1	191	46	42	0.00097	0.0874	0.0024	0.0737	0.0050	2.461	0.114	0.2042	0.0069	1,198	37	1,261	33	1,369	52	1,438	95	**1,243**	**33**
Z22-1	66	34	18	0.00335	0.0649	0.0080	0.0586	0.0082	1.974	0.261	0.2207	0.0080	1,286	42	1,107	89	770	261	1151	156	**1,268**	**42**
Z23-1	263	300	91	0.00068	0.1000	0.0014	0.0757	0.0027	3.815	0.146	0.2768	0.0094	1,575	47	1,596	31	1,623	26	1,474	51	**1,614**	**24**
Z26-1	45	4	10	0.00803	0.0578	0.0197	–	–	1.235	0.431	0.1551	0.0066	929	37	817	198	521	612	–	320	**930**	**37**
Z28-1	1182	630	271	0.00032	0.0829	0.0006	0.0656	0.0022	2.395	0.083	0.2096	0.0070	1227	37	1,241	25	1,266	13	1,284	43	**1,263**	**12**
Z29-1	111	62	29	0.00120	0.0908	0.0036	0.0706	0.0041	2.762	0.155	0.2205	0.0077	1,285	40	1,345	42	1,443	76	1,378	77	–	–
Z30-1	157	116	26	0.00059	0.0667	0.0027	0.0405	0.0019	1.362	0.078	0.1481	0.0051	890	29	873	33	830	86	803	38	**885**	**28**
Z31-1	110	68	30	0.00280	0.0900	0.0051	0.0652	0.0047	2.629	0.184	0.2119	0.0075	1,239	40	1,309	52	1,426	108	1,277	89	**1,248**	**39**
Z4-1	150	55	28	0.00120	0.0723	0.0045	0.0509	0.0050	1.682	0.125	0.1688	0.0059	1,005	32	1,002	48	994	126	1,004	97	**1,005**	**32**
Z5-1	120	43	23	0.00164	0.0704	0.0040	0.0490	0.0046	1.645	0.116	0.1694	0.0059	1,009	32	988	44	940	117	966	88	**1,005**	**32**
Z7-1	109	76	22	0.00440	0.0674	0.0088	0.0408	0.0045	1.367	0.191	0.1470	0.0053	884	30	875	82	850	274	809	88	**884**	**30**
Z8-1	147	88	50	0.00219	0.0961	0.0042	0.0666	0.0051	3.743	0.222	0.2824	0.0098	1,603	49	1,581	48	1,551	83	1,302	96	**1,590**	**44**
Z9-1	701	199	155	0.00098	0.0845	0.0013	0.0582	0.0028	2.425	0.093	0.2081	0.0069	1,219	37	1,250	28	1,305	29	1,143	54	**1,274**	**27**

The U–Pb ratios were corrected for common lead using ^{204}Pb and Broken Hill lead composition. The significant different errors of individual measurements are the consequence of different analytical conditions during both sessions (see text)

[a]Bold-marked age data were used to construct the probability curves in Figs. 4 and 6. They represent Concordia ages, which were determined according to the method of Ludwig (1998). In those cases, where more than one analysis on a single zircon grain yields discordant ages, the upper intercept age is given (italic font style)

[b]Regression line was forced through the origin

References

Åhäll K-I, Larson Å (2000) Growth-related 1.85–1.55 Ga magmatism in the Baltic Shield; a review addressing the tectonic characteristics of Svecofennian, TIB 1-related, and Gothian events. Geol Fören Förh 122:193–206

Abdelsalam MG, Liegeois J-P, Stern RJ (2002) The Saharan metacraton. J Afr Earth Sci 34:119–136

Anthes G, Reischmann T (2001) Timing of granitoid magmatism in the eastern mid-German crystalline rise. J Geodyn 31:119–143

Bankwitz P (1995) Die Erdkruste der östlichen Rhenoherzynischen Zone im Umfeld des Harzes. Zentralbl Geol Paläontol Teil I 9(10):1551–1557

Baumann A, Grauert B, Mecklenburg S, Vinx R (1991) Isotopic age determination of crystalline rocks of the Upper Harz Mountains, Germany. Geol Rundsch 80:669–690

Bevier ML, Barr SM, White CE (1990) Late Precambrian U-Pb ages for the Brookville Gneiss, southern New Brunswick. J Geol 98:955–965

Bingen B, Nordgulen Ø, Sigmond EMO, Tucker R, Mansfeld J, Högdahl K (2003) Relations between 1.19–1.13 Ga continental magmatism, sedimentation and metamorphism, Sveconorwegian province, S Norway. Precamb Res 124:215–241

Black LP, Williams IS, Compston W (1986) Four zircon ages from one rock: the history of a 3930 Ma-old granulite from Mount Sones, Enderby Land, Antarctica. Contrib Mineral Petrol 94:427–437

Boullier AM (1991) The Pan-African Trans-Saharan belt in the Hoggar shield (Algeria, Mali, Niger): a review. In: Dallmeyer RD, Lécorché JP (eds) The West African Orogens and circum-Atlantic correlations. Springer, Berlin, Heidelberg, New York, pp 85–105

Bregar M, Bauernhofer A, Pelz K, Kloetzli U, Fritz H, Neumayr P (2002) A late Neoproterozoic magmatic core complex in the Eastern Desert of Egypt: emplacement of granitoids in a wrench-tectonic setting. Precamb Res 118:59–82

Cahen L, Snelling NJ, Delhal J, Vail JR, Bonhomme M, Ledent D (1984) The geochronology and evolution of Africa. Clarendon Press, Oxford, pp 1–512

Claoué-Long JC, Compston W, Roberts J, Fanning CM (1995) Two Carboniferous ages: a comparison of SHRIMP zircon dating with conventional zircon ages and $^{40}Ar/^{39}Ar$ anayses: geochronology, time scales and global stratigraphic correlation. Soc Sed Geol Spec Publ 54:3–21

Compston W, Williams IS, Meyer C (1984) U-Pb geochronolgy of zircons from the lunar breccia 73217 using a sensitive high-resolution ion microprobe. In: Proceedings XIV lunar planetary science conference. J Geophys Res 89:B525-B534

DeLaeter JR, Kennedy AK (1998) A double focussing mass spectrometer for geochronology. Int J Mass Spec Ion Proc 178:43–50

Dick HJB, Bullen T (1984) Chromian spinel as a petrogenetic indicator in abyssal and alpine peridotites and spatially associated lavas. Contrib Mineral Petrol 86:54–76

Dickinson WR, Gehrels GE (2003) U–Pb ages of detrital zircons from Permian and Jurassic eolian sandstones of the Colorado Plateau, USA: paleogeographic implications. Sedim Geol 163:29–66

Dörr W, Zulauf G, Fiala J, Franke W, Vejnar (2002) Neoproterozoic to Early Cambrian history of an active plate margin of the Teplá Barrandian unit—a correlation of U-Pb isotope-dilution-TIMS ages (Bohemia, Czech Republic). Tectonophysics 352:65

Düweke M, Ehrismann W, Krahmer U, Rosenbach O (1976) Magnetische und gravimetrische Messungen im Kontaktbereich Eckergneis-Gabbro des Harzer Brockenplutons. Geol Jhb 6:81–108

Ermannsdörfer OH (1909) Der Eckergneis im Harz. Ein Beitrag zur Kenntnis der Kontaktmetamorphose und der Entstehung kristalliner Schiefer. Jb Königl-Preuß Geol Landesanst Bergakad Berlin 30:324–338

Fernández-Suárez J, Gutiérrez Alonso G, Jefries TE (2002) The importance of along-margin terrane transport in northern Gondwana: insights from detrital zircon parentage in Neoproterozoic rocks from Iberia and Brittany. Earth Planet Sci Lett 204:75–88

Franke W (1989) Tectonostratigraphic units in the Variscan belt of Central Europe. Geol Soc Amer Spec Pap 230:67–90

Franke W (2001) The mid-European segment of the Variscides: tectonostratigraphic units, terrane boundaries and plate tectonic evolution. Geol Soc London Spec Publ 179:35–61

Franz L, Schuster AK, Strauss KW (1997) Basement evolution in the Rhenohercynian Segment: Discontinuous exhumation history of the Eckergneis complex (Harz Mountains, Germany). Chem Erde 57:105–135

Franzke HJ (2001) Die strukturelle Einbindung des Eckergneises zu seinem variscisch geprägten Umfeld. Braunschweiger Geowiss Arb 24:1–26

Friedel CH, Hoth P, Franz G, Stedingk K (1995) Niedriggradige Regionalmetamorphose im Harz. Zbl Geol Paläont Teil 1 (1993), H 9/10:1213–1235

Gaál G, Gorbatschev R (1987) An outline of the Precambrian evolution of the Baltic Shield. Precamb Res 35:15–52

Ganssloser M (1999) Detrital chromian spinels in Rhenohercynian greywackes and sandstones (Givetian–Visean, Variscides, Germany) as indicators of ultramafic source rocks. Geol Mag 136:437–451

Gee DG, Sturt BA (1985) The Caledonide orogen—Scandinavia and related areas. Wiley, Chichester, pp 1–1266

Geisler T, Pidgeon RT (2001) Significance of radiation damage on the integral SEM cathodoluminescence intensity of zircon: an experimental annealing study. N Jb Miner Monatsh 10:433–445

Geisler T, Schleicher H (2000) Composition and U-Th-total Pb model ages of polygenetic zircons from the Vånga granite, south Sweden: an electron microprobe study. Geol Fören Förh 122:227–235

Geisler T, Ulonska M, Schleicher H, Pidgeon RT, van Bronswijk W (2001) Leaching and differential recrystallization of metamict zircon under experimental hydrothermal conditions. Contrib Mineral Petrol 141:53–65

Geisler T, Pidgeon RT, van Bronswijk W, Kurtz R (2002) Transport of uranium, thorium, and lead in metamict zircon under low-temperature hydrothermal conditions. Chem Geol 191:141–154

Geisler T, Trachenko K, Ríos S, Dove M, Salje EKH (2003a) Impact of self-irradiation damage on the aqueous durability of zircon ($ZrSiO_4$): implications for its suitability as nuclear waste form. J Phys Condens Matter 15:L597-L605

Geisler T, Pidgeon RT, Kurtz R, van Bronswijk W, Schleicher H (2003b) Experimental hydrothermal alteration of partially metamict zircon. Am Mineral 86:1496–1518

Geisler T, Rashwan AA, Rahn M, Poller U, Zwingmann H, Pidgeon RT, Schleicher H (2003c) Low-temperature hydrothermal alteration of natural metamict zircons from the Eastern Desert, Egypt. Mineral Mag 67:485–508

Geisler T, Seydoux-Guillaume A-M, Wiedenbeck M, Berndt J, Wirth R, Zhang M, Mihailova B, Putnis A, Salje EKH, Schlüter J (2004) Periodic pattern formation in hydrothermally treated, metamict zircon. Amer Mineral 89:1341–1347

Gradstein FM, Ogg JG, Smith AG, Agterberg FP, Bleeker W et al (2004) A geological timescale 2004. Cambridge University Press, Cambridge

Grauert B, Wagner ME (1975) Age of granulite-facies metamorphism of the Wilmington Complex, Delaware-Pennsyvania Piedmont. Am J Sci 275:683–691

Hallsworth CR, Morton AC, Claoué-Long J, Fanning CM (2000) Carboniferous sand provenance in the Pennine Basin, UK: constraints from heavy mineral and detrital zircon age data. Sedim Geol 137:147–185

Haverkamp J, van Hoegen J, Kramm U, Walter R (1992) Application of U–Pb systems from detrital zircons for paleographic reconstructions—a case study from the Rhenohercynian. Geo Acta 5:69–82

Huckriede H, Ahrendt H, Franke W, Wemmer K, Meischner D (1998) Orogenic processes recorded in Early Carboniferous and Devonian clastic sediments of the Rhenohercynian Zone. Terra Nostra 98(2):77–79

Ingle S, Mueller PA, Heatherington AL, Kozuch M (2003) Isotopic evidence for the magmatic and tectonic histories of the Carolina terrane: implications for stratigraphy and terrane affiliation. Tectonophys 371:187–211

Irvine TN (1967) Chromian spinel as a petrogenetic indicator Part 2: Petrologic applications. Can J Earth Sci 4:71–97

Karabinos P, Gromet LP (1993) Application of single-grain zircon evaporation analysis to detrital grain studies and age discrimination in igneous suites. Geochim Cosmochim Acta 57:4257–4267

Krohe A (1996) Variscan tectonics of central Europe: postaccretionary intraplate deformation of weak continental lithosphere. Tectonics 15:1364–1388

Kröner A, Jaecker P, Williams IS (1994) Pb-loss patterns in zircons from a high-grade metamorphic terrain as revealed by different dating methods: U–Pb and Pb–Pb ages for igneous and metamorphic zircons from northern Sri Lanka. Precamb Res 66:151–181

Ludwig KR (1998) Calculation of uncertainties of U–Pb isotope data. Earth Plan Sci Lett 46:212–220

Ludwig KR (2001) Users manual for isoplot/Ex Version 2.49. A Geochronological Toolkit for Microsoft Excel. Berkeley Geochronology Center, Special Pubication No. 1a, Berkeley.

Mohr K (1978) Geologie und Minerallagerstätten des Harzes. E Schweizerbartsche Verlgasbuchhandlung, Stuttgart, pp 1–387

Möller A, O'Brien PJ, Kennedy A, Kröner A (2002) Polyphase zircon in ultrahigh-temperature granulites SW Norway): constraints for Pb diffusion in zircon. J Metam Geol 20:727–740

Morton AC, Claoué-Long JC, Hallsworth CR (2001) Zircon age and heavy mineral constraints on provenance of the North Sea Carboniferous sandstone. Mar Petrol Geol 18:319–337

Müller G, Strauss KW (1985) Polymetamorphe Entwicklung des Eckergneis-Komplexes/Harz. N Jb Mineral Abh 152(3):271–291

Nironen M (1997) The Svecofennian Orogen: a tectonic model. Precamb Res 86:21–44

Nutman AP, McGregor VR, Friend CRL, Bennett VC, Kinny PD (1996) The Itsaq gneiss complex of southern West Greenland: the world's most extensive record of early crustal evolution (3900–3600 Ma). Precamb Res 78:1–39

Obst K, Hammer J, Katzung G, Korich D (2004) The Mesoproterozoic basement in the southern Baltic Sea: insights from the G 14–1 off-shore borehole. Int J Earth Sci 93:1–12

Oncken O (1997) Transformation of a magmatic arc and an orogenic root during oblique collision and its consequences for the evolution of the European Variscides (Mid-German Crystalline Rise). Geol Rund 86:2–20

Pharaoh TC (1999) Palaeozoic terranes and their lithospheric boundaries within the Trans-European Suture Zone (TESZ): a review. Tectonophys 314:17–41

Pidgeon RT, Furfaro D, Kennedy AK, Nemchin AA, van Bronswijk W (1994) Calibration of zircon standards for the Curtin SHRIMP II. 8th international conference on geochronology, cosmochronology and isotope geology. US Geological Survey Circular 1107:251

Pin C (1991) Central-West Europe: Major stages of development during Precambrian and Paleozoic times. In: Dallmeyer RD, Lécorché JP (eds) The West African orogens and circum-Atlantic correlations. Springer, Berlin, Heidelberg, New york, pp 295–306

Press S (1986) Detrital spinels from alpinotype source rocks in Middle Devonian sediments of the Rhenish Massif. Geol Rund 75:333–340

Reinhardt J, Kleemann U (1994) Extensional unroofing of granulitic lower crust and related low-pressure, high-temperature metamorphism in the Saxonian Granulite Massif, Germany. Tectonophys 238:71–94

Robardet M (2003) The Amorica 'microplate': fact or fiction? Critical review of the concept and contradictory paleobiographical data. Paleageogr Paleoclimatol Paleoecol 60:283–304

Rocci G, Bronner G, Deschamps M (1991) Crystalline basement of the West African craton. In: Dallmeyer RD, Lécorché JP (eds) The West African orogens and circum-Atlantic correlations. Springer, Berlin, Heidelberg, New york, pp 31–61

Schaltegger U, Fanning CM, Günther D, Maurin JC, Schulmann K, Gebauer D (1999) Growth, annealing and recrystallization of zircon and preservation of monazite in high-grade metamorphism: conventional and in-situ U-Pb isotope, cathodoluminescence and microchemical evidence. Contrib Mineral Petrol 134:186–201

Schoell M, Lenz H, Harre W (1973) Das Alter der Hauptmetamorphose des Eckergneises im Harz auf Grund von Rb/Sr-Datierungen. Geol Jb A9:89–95

Söderlund U, Jarl L-G, Persson P-O, Stephens MB, Wahlgren C-H (1999) Protolith ages and timing of deformation in the eastern, marginal part of the Sveconorwegian orogen, southwestern Sweden. Precamb Res 94:29–48

Söderlund U, Möller C, Andersson J, Johansson L, Whitehouse M (2002) Zircon geochronology in polymetamorphic gneisses in the Sveconorwegian orogen, SW Sweden: ion microprobe evidence for 1.46–1.42 and 0.98–0.96 Ga reworking. Precamb Res 113:193–225

Steiger RH, Jäger E (1977) Subcommision on Geochronology: convention on the use of decay constants in geo- and cosmochronology. Earth Planet Sci Lett 36:359–362

Strachan RA, Nutman AP, Friderichsen JD (1995) SHRIMP U-Pb geochronology and metamorphic history of the Smallefjord sequence, NE Greenland Caledonides. J Geol Soc Lond 152:779–784

Tapponier P, Lacassin R, Leloup PH, Schärer U, Dalai Z, Haiwei W, Xiaohan L, Shaocheng J, Liangshen Z, Jiayou Z (1990) The Ailao Shan-Red River metamorphic belt: Tertiary left lateral shear between Sundaland and South China. Nature 343:431–437

Tassinari CCG, Macambira MJB (1999) Geochronological provinces in the Amazonian craton. Episodes 22:174–182

Tesalina SG, Nimis P, Augé T, Zaykov VV (2003) Origin of chromite in mafic–ultramafic-hosted hydrothermal massive sulfides from the Main Uralian Fault, South Urals, Russia. Lithos 70:39–59

Tichomirowa M, Berger H-J, Koch EA, Belyatski BV, Götze J, Kempe U, Nasdala L, Schaltegger U (2000) Zircon ages of high-grade gneisses in the Eastern Erzgebirge (Central European Variscides)—constraints on origin of the rocks and Precambrian to Ordovician magmatic events in the Variscan foldbelt. Lithos 56:303–332

Tomaschek F, Kennedy AK, Villa IM, Lagos M, Ballhaus C (2003) Zircons from Syros, Cyclades, Greece—Recrystallization and mobilization of zircon during high-pressure metamorphism. J Petrol 44:1977–2002

Torsvik TH (1998) Palaeozoic palaeogeography: a North Atlantic viewpoint. Geol Fören Förh 120:109–118

Vavra G, Gebauer D, Schmid R, Compston W (1996) Multiple zircon growth and recrystallization during polyphase Late Carboniferous to Triassic metamorphism in granulites of the Ivrea Zone (Southern Alps): an ion microprobe (SHRIMP) study. Contrib Mineral Petrol 122:337–358

Vavra G, Schmid R, Gebauer D (1999) Internal morphology, habit and U–Th–Pb microanalysis of amphibolite-to-granulite facies zircons: geochronology of the Ivrea Zone (Southern Alps). Contrib Mineral Petrol 134:380–404

Vermeesch P (2004) How many grains are needed for provenance study. Earth Planet Sci 224:441–451

Wachendorf H (1986) Der Harz—Variszischer Bau und geodynamische Entwicklung. Geol Jhb A 91:3–67

Wachendorf H, Buchholz P, Zellmer H (1995) Fakten zum Harz-Paläozoikum und ihre geodynamische Interpretation. Nova Acta Leopoldina NF 71 Nr 291:119–150

Willner AP, Krohe A, Maresch MV (2000) Interrelated P–T–t–d paths in the Variscan Erzgebirge dome (Saxony, Germany): Constraints on the rapid exhumation of high-pressure rocks from the root zone of a collisional orogen. Int Geol Rev 41:64–85

Zeh A, Brätz H, Millar IL, Williams IS (2001) A combined zircon SHRIMP and Sm–Nd isotope study of high-grade paragneisses from the Mid-German Crystalline Rise: evidence for northern Gondwana and Grenvillian provenance. J Geol Soc London 158:983–994

Zhao G, Cawood PA, Wilde SA, Sun M (2002) Review of global 2.1–1.8 Ga orogens: implications for a pre-Rodinia supercontinent. Earth Sci Rev 59:125–162

Zulauf G, Dörr W, Fiala J, Vejnar Z (1997) Late Cadomian crustal tilting and Cambrian transtension in the Teplá-Barrandian unit (Bohemian Massif, Central European Variscides). Geol Rundsch 86:571–584